

Rising Temperature Trends across the Narayani River Basin in Central Nepal Projected by CMIP6 Models

Aabiskar Timilsina^a, Rocky Talchabhadel^b, Vishnu Prasad Pandey^c

^{a, c} Department of Civil Engineering, Pulchowk Campus, IOE, Tribhuvan University, Nepal

^b Texas A&M AgriLife Research, Texas A&M University, El Paso, USA

Corresponding Email: ^a aabiskar.er@gmail.com

Abstract

A sound understanding of projected climate, including precipitation and temperature, is critical for an effective design and planning of adaptation and mitigation measures in combating the adverse effects of climate change. This study projects maximum (T_{max}) and minimum (T_{min}) daily temperature in the Narayani River Basin (NRB), central Nepal, for three future periods, namely, near (NF: 2021-2045), mid (MF: 2046-2075), and far (FF: 2076-2100). Three Global Climate Models (GCMs) were chosen from ten Coupled Model Inter-comparison Project Phase 6 (CMIP6) GCMs under two shared socioeconomic pathways, SSP245 (4.5 Watt/m²) and SSP585 (8.5 Watt/m²). The selected GCMs were bias-corrected using a linear transfer function after exploring several methods. Two statistical tests, i.e., Sen's Slope and Mann-Kendall, were employed to quantify the magnitude, direction, and significance of monotonic trends. Multi-model Ensemble (MME) of selected GCMs demonstrated a widespread and significant rising trend across the basin at all seventeen meteorological stations, with very few exceptions. The average annual T_{max} across the NRB is projected to increase by ranging from 0.08°C to 1.09°C for NF, 0.74°C to 1.58°C for MF, and 1.45°C to 2.15°C for FF under the scenario SSP245. Similarly, under SSP585, the T_{max} will increase ranging from 0.6°C to 1.40°C for NF, 1.26°C to 2.31°C for MF, and 2.90°C to 4.68°C for FF with respect to (wrt) the historical period (1980-2014). For T_{min} under SSP245, is projected to increase ranging from 0.39°C to 1.24°C for NF, 1.53°C to 2.74°C for MF, and 1.85°C to 3.20°C for FF. Similarly, under SSP585, the T_{min} is projected to increase ranging from 0.42°C to 1.46°C for NF, 2.08°C to 3.82°C for MF, and 3.30°C to 5.22°C for FF wrt the historical period. Furthermore, varying trends are expected across the seasons, in particular, higher deviation during winter (0.9°C to 5.4°C) followed by pre-monsoon (-0.1°C to 2.8°C) for T_{max} while winter (0.8°C to 3.7°C) followed by post-monsoon (1.1°C to 4.1°C) for T_{min} is seen across the basin. Our results indicated that the warming trend is more pronounced for the mountainous region, likely affecting high altitudes' snow and glacier cover. These bias-corrected projections of T_{max} and T_{min} can be used for climate change impact assessment in hydrology, water resources, and other sectors in the NRB.

Keywords

Climate Change, Coupled Model Inter-comparison Project Phase 6 (CMIP6), Global Climate Model (GCM), Narayani River Basin (NRB)

1. Introduction

Global temperatures have risen dramatically over the last decades due to various natural and anthropogenic variability [1]. The research on global temperature based on data from 1951 to 2012 revealed that there is warming trend in global temperature and the temperature is increasing at the rate of 0.12 °C per decade [2]. River basins worldwide are being impacted to varying degrees by climate change [3, 4].

Recent study over south Asian countries using latest CMIP6 GCMs showed that, at the end of the 21st century, the annual mean temperature will be increased by 2.1°C under SSP245 and 4.3°C under SSP585[5]. Since large areas of the Himalayas are covered in snow and glaciers, and the region is very sensitive to global warming [6].

Like many other countries, Nepal is facing a significant warming trend of temperature, which has a huge influence on snow and glaciers, which further

affects melt water dependent river system [7, 8]. Some of the studies on future climate projection have been carried on the Koshi river basin [9, 10, 11, 12] and the Bagmati river basin [10]. The study by Nepal et al. (2016) in the Koshi river basin showed that there would be 4 °C increase in temperature by the end of the century. Furthermore, they highlighted that there would be an increase in T_{\min} and T_{\max} of both seasonal and annual temperature throughout the century. The temperature of the coldest day, coldest night, warmest day, and warmest night are also expected to increase in the Koshi River Basin [6]. Similarly, in western Nepal, the temperature is rising [13]. Dahal et al. (2020) showed that the Karnali River Basin had a similar increasing trend throughout the basin [9].

As the Narayani River Basin (NRB) is a part of large Hindu-Kush Himalayan (HKH) region, a mountainous environment can be greatly affected by the change in temperature posing enormous challenge for large human population and environment depending on their resources. The trend analysis of the observed historical data from various meteorological stations showed the warming trend of 0.028 °C per year (yr^{-1}) to 0.035 °C yr^{-1} with a mean increasing trend of 0.03 °C yr^{-1} in NRB [14]. This type of warming will lead to changes in the availability of water, especially in spring and autumn. Furthermore, seasonal temperature changes will also significantly affect agricultural production by increasing the stress on the crop [15]. Therefore, the study of temporal and spatial changes in temperature is essential to assess climate change, especially in the Himalayas, where billions of people living downstream depend on the water produced by melting snow and glaciers. Therefore, the analysis of future temperature predictions and related uncertainties is well suited for adaptation planning.

The Global Climate Models (GCMs) can provide a better understanding of the region's future climate based on emission scenarios known as the Socio-economic Pathways (SSPs). In the IPCC's Sixth Assessment Report (AR6) based on the Coupled Model Intercomparison Project Phase 6 (CMIP6), the shared socioeconomic pathways (SSPs) are used for future climate projections; these scenarios can be used to project future temperature with high confidence [16]. The Multi-model Ensemble (MME) is generally used to avoid the uncertainties presented in different GCMs [17], generated by selecting the few

best-performed GCMs from a pool of GCMs [18]. However due to the coarse spatial resolution of GCMs, required to correct biases while using in regional scales. The process of escalating the quality of climate outputs by reducing the systematic errors to improve their fittings to observations is called bias correction. There are several various bias correction methods available [19]. The selection of the suitable bias correction method is essential in assessing future climates [20].

This study aims to estimate projected changes in future temperature in the NRB based on bias-corrected multiple CMIP6 model outputs under two future scenarios, namely, SSP245 and SSP585. The specific objectives are three folds: i) to select a set of suitable GCMs and bias correction method for the NRB; ii) to project the daily time series of maximum and minimum temperature for three future periods, namely, near-future (NF: 2021-2045), mid-future (MF: 2046-2075), and far-future (FF: 2076-2100); and iii) to detect the trends in projected future temperatures, annual as well as seasonal.

2. Study Area and Data

2.1 Study Area

The NRB, also known as Gandaki River Basin, is located in central Nepal and extends from 27°21' to 29°20' latitude and 82°53' to 86°13' longitude. The NRB is the sub basin of the Ganges River Basin. This study only encompasses the Nepalese part (32,104 km^2) [15] of the basin. The NRB is bounded by the Karnali basin to the west and the Koshi basin to the east. The NRB includes the Himalayan range to plains of terai, with the elevation varying from 18 m in the south to higher than 8000 m to the Himalayas with mean elevation of 4065 m above sea level (asl) including different physiographic regions i.e Hill, Mountain and High Himalayas including trans-Himalaya [21]. The temperature varies rapidly with elevation like the recorded T_{\min} in the high Himalayas is -25°C, while the recorded T_{\max} in plains of terai is 35°C [22]. Narayani River is a perennial, torrential, turbulent and undisturbed river that originates from the Himalayas at the lower edge of the Tibetan Plateau and carries snow-fed flows with significant discharge even in the dry period. The seven major tributaries of Narayani River are Marsyangdi, Daraudi, Seti, Madi, Kali Gandaki, Budhi Gandaki, and Trishuli [14]. The river is being

Rising Temperature Trends across the Narayani River Basin in Central Nepal Projected by CMIP6 Models

used for irrigation at various locations and its major tributaries are also being used for hydropower, water supply and irrigation purpose. Its final outlet point is gauged at Narayanghat, Chitwan. The area of the NRB considered in this study is shown in Figure 1.

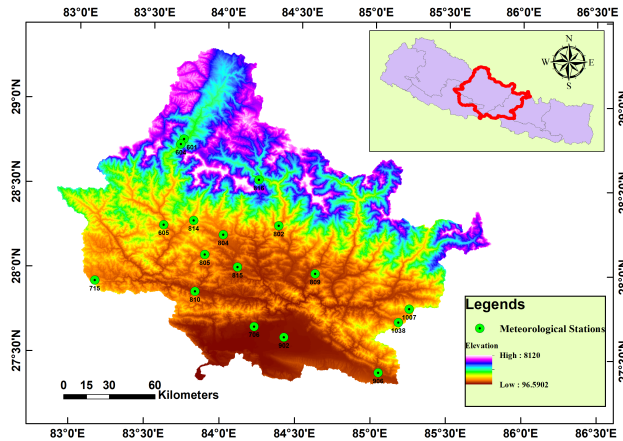


Figure 1: Location, topography, and selected meteorological stations in the Narayani River Basin

2.2 Data and Sources

2.2.1 Temperature Data

Observed historical data of daily T_{max} and T_{min} of thirty-one meteorological stations are available for NRB at Department of Hydrology and Meteorology (DHM), Government of Nepal, from 1981 to 2014. However, there is a lack of reliable data for adequate record length. The stations with more than 20% missing values were avoided in this study. As a result, only seventeen stations were selected considering the inclusion of all three physiographic regions (i.e., Mountains, Hills, and Terai) and maintaining a proper spatial distribution to represent the whole basin. Details of the selected meteorological stations are presented in Table 1.

2.2.2 GCMs (CMIP6) Data

This study used historical (1980-2014) data and future (2015-2100) projections of CMIP6 GCMs for T_{max} and T_{min} . The temperature variables such as T_{max} and T_{min} of the SSP are established based on a certain level of radiative forcing related to emissions, land-use scenarios, and social concerns. The CMIP6 has been significantly improved compared to the previous CMIP5 as it offers socio-economic pathways [23]. We obtained daily T_{max} and T_{min} from 10 CMIP6-GCMs (Table 2) from <https://esgf-node.llnl.gov/search/cmip6/> for two scenarios ssp245 and ssp585.

3. Methodology

The overall methodology of this study is shown in Figure 2. The major activities involved are the acquisition of observed data and GCMs data set, selection of stations for observed data and selection of few GCMs based on performance, choice of best-performed bias correction method, projection of future bias-corrected daily T_{max} and T_{min} , trend analysis of annual mean temperature, seasonal and monthly change in temperature of different future periods. The future period 2021-2100 was divided into three future periods as NF (2021-2045), MF (2046-2075), and FF (2076-2100). The details of these steps are further explained below.

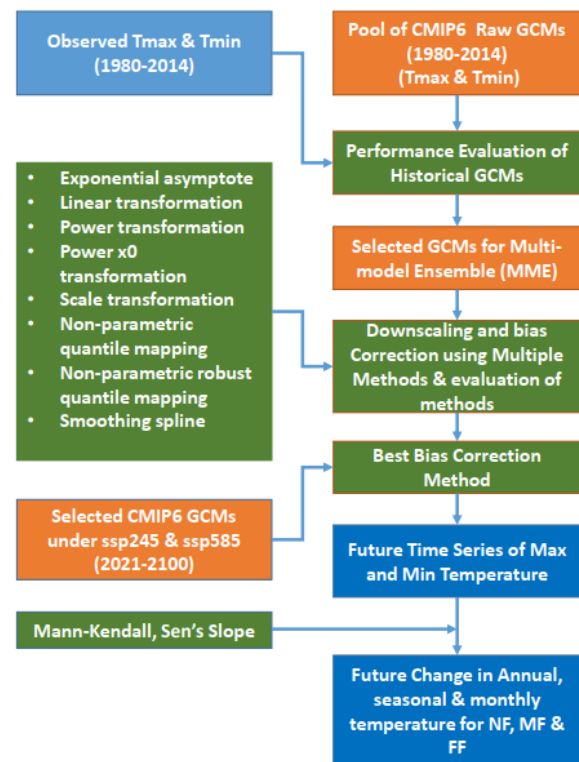


Figure 2: Methodological flowchart of the study (NF: Near Future (2021-2045); MF: Mid Future (2046-2075); FF: Far Future (2076-2100))

3.1 Observational Data Gap Filling

The daily data from selected DHM stations were visually inspected for the period 1980 to 2014 to find out the gap in the data using time series plots. The percentage of missing data ranges from 0 to about 80% in various stations. The missing data were filled using the long-term average method for the months with missing data less than 10 consecutive days. However for the months with missing data more than

Table 1: List of meteorological stations used in this study C is Climatology; A is Agrometeorology and An is Aeronautical for types of the basin)

SN	Station Name	Index No.	Station Type	District	Latitude (Deg)	Longitude (Deg)	Elevation (m)
1	Jomsom	601	C	Mustang	28.78	83.72	2744
2	Thakmarpha	604	A	Mustang	28.75	83.70	2566
3	Baglung	605	C	Baglung	28.26	83.60	984
4	Dumkauli	706	A	Nawalparasi	27.68	83.21	154
5	Khanchikot	715	C	Argkhanchi	27.93	83.15	1760
6	Khudi Bazar	802	C	Lamjung	28.28	84.36	823
7	Pokhara Airport	804	An	Kaski	28.21	84.00	827
8	Syangja	805	C	Syangja	28.10	83.15	868
9	Gorkha	809	A	Gorkha	28.00	83.61	1097
10	Chapkot	810	C	Syangja	27.88	81.81	460
11	Lumle	814	A	Kaski	28.30	83.80	1740
12	Khairini Tar	815	A	Tanahun	28.03	84.10	500
13	Chame	816	C	Manang	28.55	84.23	2680
14	Rampur	902	A	Chitwan	27.61	84.41	256
15	Hetauda NFI	906	C	Makwanpur	27.41	85.05	474
16	Kakani	1007	A	Nuwwakot	27.80	85.25	2064
17	Dhunibesi	1038	C	Dhanding	27.71	85.18	1085

consecutive 10 days were filled using the data produced over Nepal by Asian Precipitation Highly Resolved Observational Data Integration Towards Evaluation of Water Resources (APHRODITE) [24]. Since only the average temperature was available in APHRODITE, the mean deviation of T_{max} and T_{min} were calculated from observed mean monthly data with respect to the APHRODITE mean monthly data. The calculated mean deviation was used to calculate respective T_{max} and T_{min} temperatures from the available average temperature.

3.2 GCMs Selection

Ten GCMs for T_{max} and T_{min} were selected to form a pool of raw GCMs that participated in the CMIP6. Taking several GCMs helps to minimize the uncertainty present in GCMs and 10 is well enough to form a initial pool. The 10 GCMs were selected based on the availability of daily T_{max} and T_{min} for historical and two future scenarios ssp245 and ssp585, and mostly used for the South Asian region’s climate change study [25]. Three performance metrics (i.e., RSR, PBIAS, and NSE) [26] were used to evaluate the historical raw GCMs. Observed historical monthly mean T_{max} and T_{min} (1980-2014) used as a reference for performance evaluation. The performance rating was assigned to each GCM based on the criteria fixed by Moriasi et al., 2007. The average rating was

calculated from all the stations for each GCM. Finally, the three highest-rated GCMs were used for further bias correction and multi-model ensemble, each for T_{max} and T_{min} .

3.3 Bias Correction Methods

Bias correction helps to reduce the systematic errors present in climate model and helps to improve their fitting to observations. The bias correction approach modifies the expected raw daily GCM output using the difference in mean and variability between GCM and reference period observations [27]. Several bias correction methods exist [19]. The various techniques vary from simple methods to complex methods. Some of the generally used methods are linear scaling, quantile mapping (QM), analog methods, delta change method, monthly mean correction, multiple regression, gamma-gamma transformation, power transformation (PT) and so on [28, 29, 30, 19, 31].

In this study we have used the following parametric and non-parametric transfer functions to correct biases of historical (1980-2014) daily T_{max} and T_{min} of selected GCMs using the DHM temperature as reference data. In the context of this paper, T_o and T_m denote observed and modeled temperature respectively. Following [32], this transformation can

Table 2: List of climate models used in this study along with horizontal resolution, country of origin, and research center

SN	Model Name	Country	Latitude (Deg)	Longitude (Deg)	Research Centre
1	MRI-ESM2-0	Japan	1.1215	1.125	Meteorological Research Institute (MRI)
2	BCC-CSM2-MR	China	1.1215	1.125	Beijing Climate Center (BCC)
3	INM-CM4-8	Russia	1.5	2.0	Institute for Numerical Mathematics (INM)
4	INM-CM5-0	Russia	1.5	2.0	Institute for Numerical Mathematics (INM)
5	NorESM2-MM	Norway	0.9424	1.25	Norwegian Climate Center
6	MPI-ESM1-2-LR	Germany	1.865	1.875	Max Planck Institute for Meteorology (MPI)
7	MPI-ESM1-2-HR	Germany	0.9351	0.9375	Max Planck Institute for Meteorology (MPI)
8	ACCESS-ESM1-5	Australia	1.500	1.875	Australian Community Climate and Earth System Simulator (ACCESS)
9	ACCESS-CM2	Australia	1.250	1.875	Australian Community Climate and Earth System Simulator (ACCESS)
10	EC-Earth3	Europe	0.7018	0.7031	European Community Earth (EC Earth)

in general, be formulated as:

$$T_0 = h(T_m) \quad (1)$$

The probability integral transform uses the statistical transformation and forms the required distribution of variables, the transformation is defined as:

$$T_0 = F_0^{-1}(F_m(T_m)) \quad (2)$$

where, F_m is the CDF of T_m and F_0^{-1} is the inverse CDF (or quantile function) corresponding to T_0 . The parametric functions used in this study are shown below:

$$T_0 = bT_m^c \quad (3)$$

$$T_0 = a + bT_m \quad (4)$$

$$T_0 = (a + bT_m)(1 - e^{-T_m/r}) \quad (5)$$

$$T_0 = bT_m \quad (6)$$

$$T_0 = b(T_m - x_0)^c \quad (7)$$

$$T_0 = (a + bT_m)(1 - e^{-(T_m - x_0)/r}) \quad (8)$$

where, T_0 indicates the best estimate of T and a , b , c , x , and r , are free parameters subject to calibration. The transformations include power transformation (3), linear transformation (4), exponential tendency to an asymptote (5), simple scaling (6), power transformation with parameter x (7), and exponential tendency to an asymptote with parameter x (8).

Other non-parametric functions used are empirical quantile (QUANT), robust empirical quantile (RQUANT), and smoothing spline methods. The bias-corrected individual mean monthly temperatures for the baseline period (1980-2014) from the three selected GCMs were compared to that of DHM observed mean monthly temperatures to calculate performance metrics RSR, PBIAS, and NSE and rating to each method according Moriasi et al. (2007) to recognize best performing bias correction method.

3.4 Future Temperature Projection

The future daily temperature at 17 stations was projected based on an ensemble of three GCMs selected from a pool of 10 CMIP6 GCMs by examining the performance of the CMIP6 models against observed temperature data collected from DHM. The temperature projection was made for T_{max} and T_{min} under the future emission scenarios SSP245 and SSP585 for three future periods, namely, near (2021-2045), mid (2046-2075), and far (2076-2100). These future periods are considered in accordance with the climate change impact study in Chamelia

watershed of Mahakali basin by Pandey et al. [2019] [33]. A linear transfer function available as “qmap” in the R package was used as the method for bias correction as it performed the best among others. The change in average annual temperature in future periods was determined by subtracting the projected average annual temperature of each selected individual GCMs and MME. The change in seasonal temperature were calculated for four seasons named as winter (DJF), pre-monsoon (MAM), monsoon (JJAS), and post-monsoon (ON). To calculate change the average seasonal T_{max} and T_{min} are compared with the baseline (1980-2014) average seasonal temperature.

3.5 Estimation of Trends in Projected Future Time Series

The non-parametric Mann-Kendall test (Mann 1945; Kendall 1975) was used to determine the significance of annual T_{max} and T_{min} trends. This test is a statistical test is universally accepted to analyze the trend in hydro-climatological time series [34]. Using this test have two benefits, the first one is that since this test is a non-parametric test so it does not require the normally distributed data. Another one is this test has low sensitivity to abrupt breaks due to non-homogeneous time series. For non-detects data, a value that is lower than the lowest measured value among given data set is assigned. In contrast to the alternative hypothesis H_1 , the null hypothesis H_0 used in this test assumes that there is no trend(the data is independent and randomly ordered) [34]. The significance level of 5% and 10% were applied to get the significance of the trend. The trend with a significance level of 5% was abbreviated as S_1 , and the trend with a significance level of 10% was abbreviated as S_2 .

Sen’s slope [35] was applied to get the slope of the trend. This is the non-parametric procedure for estimating the slope of the trend of N pairs of data. Sen’s slope estimator has been widely used in hydro-meteorological time series [36, 37].

4. Results and Discussion

4.1 Selection of GCMs for Multi-Model Ensemble

Based on the three performance metrics (i.e., RSR, PBIAS, and NSE), the rating of each of the 10 GCMs

in the pool was assigned. A summary of the obtained average ratings is shown in Figure 3. Results showed that INM-CM4-8, INM-CM5-0, and MPI-ESM1-2-HR are the models with generally higher ratings for the T_{max} ; MRI-ESM2-0, NorESM2-MM, and MPI-ESM1-2-HR have higher ratings for T_{min} . The GCMs mentioned above were selected for further generation of MME by taking the arithmetic mean after the bias correction.

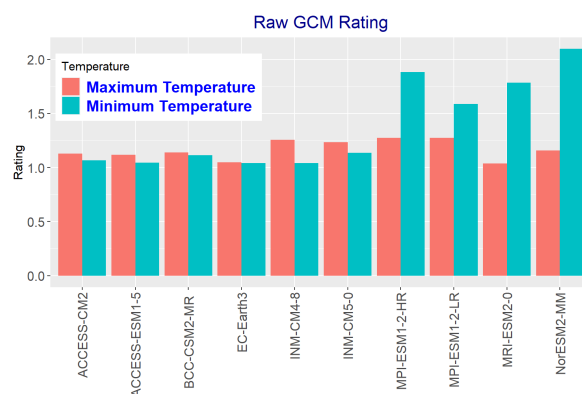


Figure 3: Average rating of the 10 GCMs for temperature data to select few GCMs for multi-model ensemble

4.2 Selected Bias Correction Methods

Nine bias correction methods were applied to correct biases present in the selected historical raw GCMs. The biases present in raw GCMs were reduced substantially after the application of these methods. Then bias-corrected GCMs daily data were compared with observed data collected from DHM to calculate three performance metrics NSE, RSR, and PBIAS. Exponential asymptote, exponential asymptote x0, and linear transfer functions outperformed the remaining methods. Among these three best-performing methods, linear transfer function showed a slightly higher rating than the other two, so chosen as the best performing bias correction method for bias correction of both T_{min} and T_{max} in that region. The rating obtained for each bias correction method for different stations is shown in Figure 4.

4.3 Projected Future Temperature

Future temperatures (2021-2100) were projected under SSP245 and SSP585 future emission scenarios on a daily time scale for seventeen weather stations in NRB. The projected annual time series of temperature tends to increase towards the final years of this century for both T_{max} and T_{min} (Figure 5). The

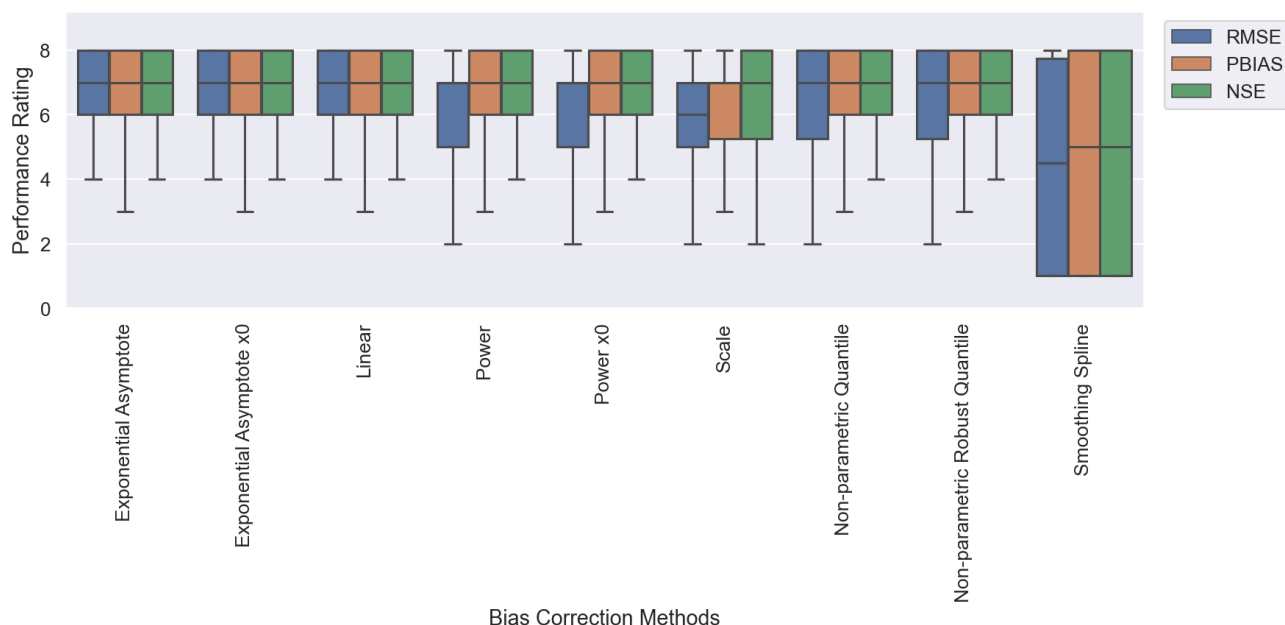


Figure 4: Rating of different bias correction functions for temperature bias correction based on performance metrics RSR, PBIAS, and NSE (Note: The ends of the box are upper and lower quartiles, horizontal line in the center of the box is for median value, and the whisker shows highest and lowest ratings)

increase rate in temperature is higher for scenario SSP585 than SSP245 for all the selected GCMs and MME. No clear pattern of future annual temperature changes was observed in future temperature change. The rate of change in future temperature is different for different models; however, large variations exist for MPI-ESM1-2-HR for both T_{max} and T_{min} . As an example, a plot of the annual time series of T_{max} at station 706 (Dumkauli) is shown in Figure 5.almazroui et al. [5] also found the similar increasing pattern in increase in temperature over south Asian countries. The temperature increases consistently with the higher forcing and over time. This is an expected result, because climate sensitivity is significantly different between models, and the impact on the model response is greater in higher scenarios and later period.

4.3.1 Annual Trend of Historical Temperature

There is a warming trend in the majority of the stations for T_{max} and T_{min} , as shown in Table 3. A significant warming trend was found in six and ten stations at a 95% significance level for T_{max} and T_{min} . The mean warming trends of $0.037^{\circ}\text{C yr}^{-1}$ and $0.022^{\circ}\text{C yr}^{-1}$ for T_{max} and T_{min} were found, which are congruous with the previous study of trend analysis of mean temperature in NRB by [14].

Table 3: Mean annual temperature trend ($^{\circ}\text{C yr}^{-1}$) of observed (1980–2014) maximum and minimum temperature for 17 stations. ‘**’ represents statistically significant at 95% significance level

Station Index	Station Name	Tmax Trend	Tmin Trend
601	Jomsom	0.0209	0.0474
604	Thakmarpha	0.0708*	0.0457
605	Baglung	-0.0365	-0.0072
706	Dumkauli	-0.0038	0.0137*
715	Khanchikot	0.0692	0.0335*
802	Khudi Bazar	0.0614*	0.0472*
804	Pokhara Airport	0.0385*	0.0349*
805	Syangja	0.0127	0.0381*
809	Gorkha	0.1026*	0.0220*
810	Chapkot	0.0080	0.0067
814	Lumle	0.0638*	0.0075
815	Khairini Tar	0.0257	0.0409*
816	Chame	0.1414*	-0.0773*
902	Rampur	-0.0053	0.0445*
906	Hetauda	0.0445	0.0153
1007	Kakani	0.0039	0.0471*
1038	Dhunibesi	0.0229	0.0193

4.3.2 Annual Trend of Projected Future Temperature

The overall result suggests significant and widespread warming trends under both scenarios for T_{max} and

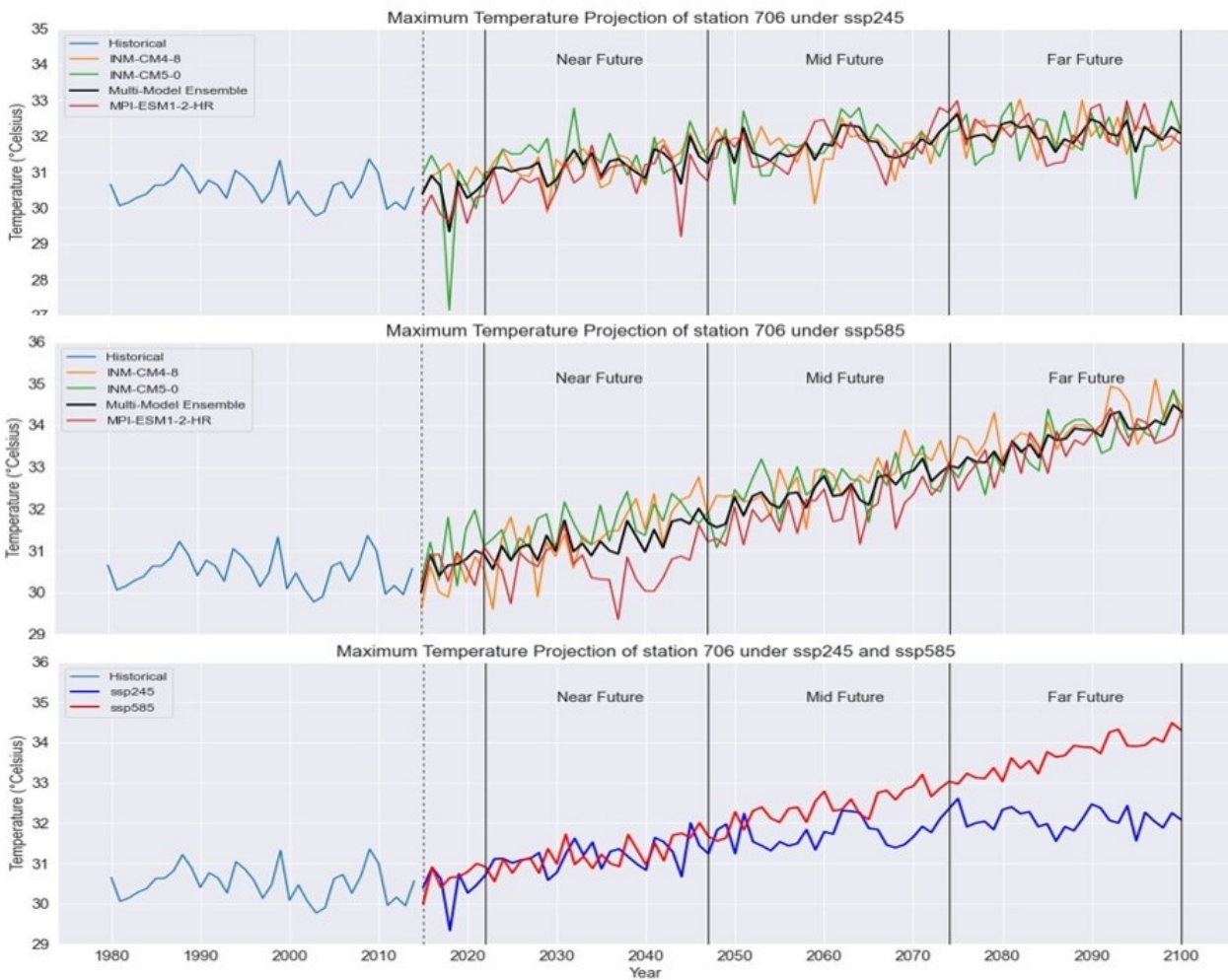


Figure 5: Time series of projected daily temperature under SSP245 and SSP585 for meteorological station 706

T_{min} . More than 80% of the trend was found to be a warming trend with significance level S_1 for almost all stations. The trend was said to be constant at that weather station if the change in temperature at that future period is within $\pm 0.001^\circ\text{C}$.

Under the scenario ssp245 in the NF for T_{max} , three GCMs except MPI-ESM1-2-HR indicated an increasing trend in the majority of the stations over that period. MPI-ESM1-2-HR indicated a constant trend in general and decreasing trend in some stations. In the mid future period, INM-CM4-8 showed an increasing trend with about 50% of stations with a significance level of S_1 , INM-CM5-0 showed majority stations with a constant trend and some stations with an increasing trend at the significance level of S_2 . Under scenario SSP585 for T_{max} in the near future, the INM-CM4-8 GCM showed a constant trend for almost 70% of the stations. All other GCMs showed an increasing trend with significance level S_1 for almost all stations. In the mid future period, the trend

was observed as an increasing trend for all other GCMs except MPI-ESM1-2-HR, which showed a constant trend for almost 50% of the considered stations. The trend in the far future period is rising with a significance level of S_1 for all the GCMs at all stations.

Under the SSP245, the T_{min} showed an increasing trend with a significant level of S_1 in the near future, except NorESM2-MM that showed an increasing trend for mountainous and some hilly stations and a constant trend for other stations. On the other hand, in the mid future period, the MRI-ESM2-0 GCM showed a constant and decreasing trend in almost equal proportions, and all the other GCMs showed an increasing trend with an S_1 significance level. Whereas, under the SSP585, the T_{min} showed an increasing trend with a significance level of S_1 for all the GCMs at all stations.

Based on the MME, the mean annual trend is 0.06°C

yr⁻¹ in NF, 0.04°C yr⁻¹ in MF, and 0.02°C yr⁻¹ in FF for T_{max} under SSP245. Similarly, 0.05°C yr⁻¹ in NF, 0.07°C yr⁻¹ in MF, and 0.1°C yr⁻¹ in FF are obtained under SSP585 for T_{max}. Also, the magnitude of mean annual trend is 0.07°C yr⁻¹ in NF, 0.04°C yr⁻¹ in MF, and 0.02°C yr⁻¹ in FF for T_{min} under SSP245. Similarly, 0.06°C yr⁻¹ in NF, 0.07°C yr⁻¹ in MF, and 0.09°C yr⁻¹ in FF are obtained under SSP585 for T_{min}. Thus, the overall results indicate that for both climate scenarios ssp245 and ssp585, the increase in future T_{max} and T_{min} is more than the historical trend obtained for the baseline period (1980-2014). The sample plot for the likely trend in NF is shown in Figure 6.

4.3.3 Projected Change in Average Annual Temperature

The spatial distribution of the projected changes in the annual mean of T_{max} and T_{min} over the NRB for three future periods under two scenarios SSP245 and SSP585 were analyzed. The anticipated change in future temperature under the SSP245 showed that T_{max} could change ranging from 0.08°C to 1.09°C for NF, 0.74°C to 1.58°C for MF, and 1.45°C to 2.15°C for FF. Similarly, under the SSP585 the T_{max} can change ranging from 0.6°C to 1.40°C for NF, 1.26°C to 2.31°C for MF, and 2.90°C to 4.68°C for FF. The anticipated change in future temperature under the SSP245 shows that T_{min} can change ranging from 0.39°C to 1.24°C for NF, 1.53°C to 2.74°C for MF, and 1.85°C to 3.20°C for FF. Similarly, under the SSP585 the T_{min} can change ranging from 0.42°C to 1.46°C for NF, 2.08°C to 3.82°C for MF, and 3.30°C to 5.22°C for FF. The sample plot of projected change in average annual temperature in NF is shown in Figure 7.

The various other studies done for this region showed similar type of result. The study done over six South Asian countries including Nepal using CMIP6 GCMs also showed warming trend across this region. According to their result by the end of this twenty-first century, the annual mean temperature is going to increase by 2.1°C under SSP245 and 4.3°C under SSP585, which is in similar pattern with the result obtained from this study [5]. According to Chhetri (2010) analysis, the rise in temperature by 1°C, 2°C, 3°C and 4°C can reduce snow cover and glaciers area by 20%, 40%, 58% and 70% respectively. Since there is large snow and glacier cover area in the NRB will have influence in runoff and water availability in

future time periods. The temperature varies largely with altitude in the NRB. The meteorological stations in high altitude in the basin are very few and the recorded data consists of large gaps. Higher number of meteorological stations with adequate and accurate data would have result better output.

4.3.4 Projected Change in Average Seasonal Temperature

All models show an increase in temperature for all seasons until the end of the century for T_{max}. The pre-monsoon (MAM) and winter (DJF) temperatures increase significantly than in the other two seasons. The value of the increase in temperature from the baseline value is large for the FF period than the other two future periods. The seasonal and annual change in T_{max} for sample station 802 is shown in Table 4.

Table 4: Projected changes (°C) in future maximum temperature at st802 based on the ensemble of three GCMs

		DJF	MAM	JJAS	ON	Average Annual
	Baseline(°C)	21.3	28.8	30.3	26.3	26.7
SSP245	NF	0.9	-0.1	1.0	1.3	0.85
	MF	1.4	0.8	1.4	1.5	1.16
	FF	2.0	1.6	1.5	1.3	1.80
SSP585	NF	1.2	-1.5	2.2	1.0	1.00
	MF	3.0	1.6	1.9	1.7	1.80
	FF	5.4	2.8	2.7	2.6	3.80

Also, there is an increase in temperature for all seasons until the end of the century for T_{min}. The winter (DJF) and post-monsoon (ON) temperatures increase significantly than in the other two seasons. The value of an increase in temperature from the baseline value is large for the FF period than the other two future periods. The seasonal and annual change in T_{min} for sample station 802 is shown in Table 5.

Our result showed that for both T_{max} and T_{min} the winter season will highly affected since increase in temperature is more for this season. Almazroui et al.(2020) also indicated that there is higher warming trend in winter season over south Asian countries. The increase in temperature may affect the snow cover area in the basin as well as the winter cropping pattern.

Likely Trend in Near Future Under ssp245

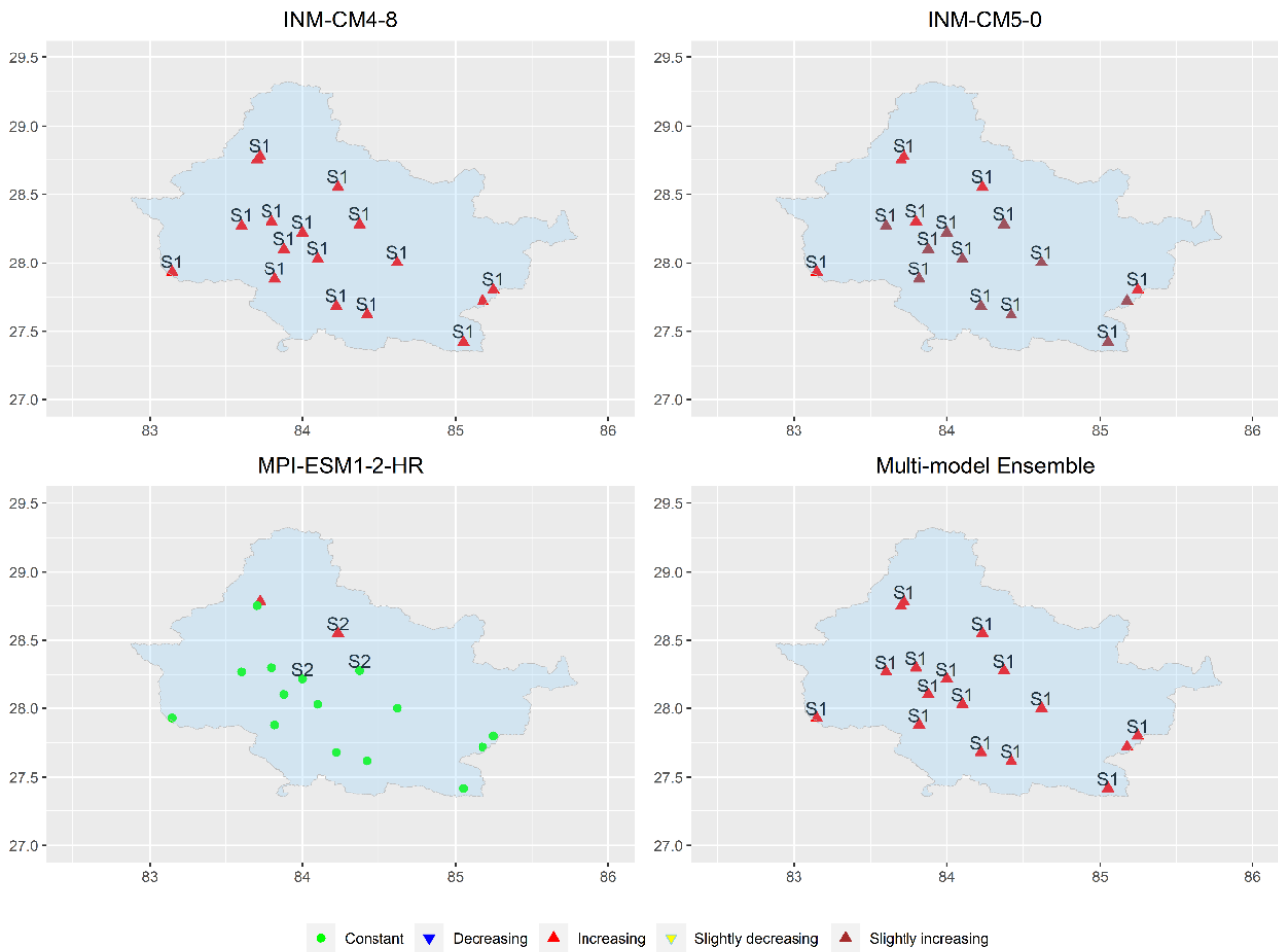


Figure 6: Trend of maximum temperature in Near Future (NF) under SSP245 (S1 is for a significance level of $\alpha = 0.05$, S2 is for a significance level of $\alpha = 0.1$ and others are not significant)

Table 5: Projected changes (°C) in future minimum temperature at st802 based on the ensemble of three GCMs

	DJF	MAM	JJAS	ON	Average Annual	
Baseline(°C)	7.8	20.5	13.2	14.2	15.5	
SSP245	NF	0.8	0.7	1.1	1.1	0.90
	MF	1.4	2.2	2.1	1.8	1.80
	FF	2.1	2.8	2.4	2.0	2.40
SSP585	NF	0.8	0.8	1.3	1.3	1.00
	MF	2.3	2.9	2.8	2.5	2.50
	FF	3.7	5.0	4.5	4.1	4.20

5. Summary and Conclusion

This study projected future temperature, both T_{max} and T_{min} , in NRB under two SSPs, SSP245 and

SSP585, and based on CMIP6 GCMs. Three GCMs from a pool of ten were identified and selected based on their performance matrix and associated ratings. The selected GCMs for T_{max} were INM-CM4-8, INM-CM5-0, and MPI-ESM1-2-HR. Similarly, for T_{min} , MRI-ESM2-0, NorESM2-MM, and MPI-ESM1-2-HR were selected. The outputs of the selected GCMs were bias-corrected using nine methods, and the most suitable method was identified as linear transfer function based on its performance. Therefore, bias-corrected results from this method were selected for preparing a MME to project future temperatures.

The future climate was projected for three future periods, namely, NF (2021-2045), MF (2046-2075), and FF (2076-2100). The result obtained from trend analysis of mean annual temperature data indicated a significant warming trend in T_{max} and T_{min} . The

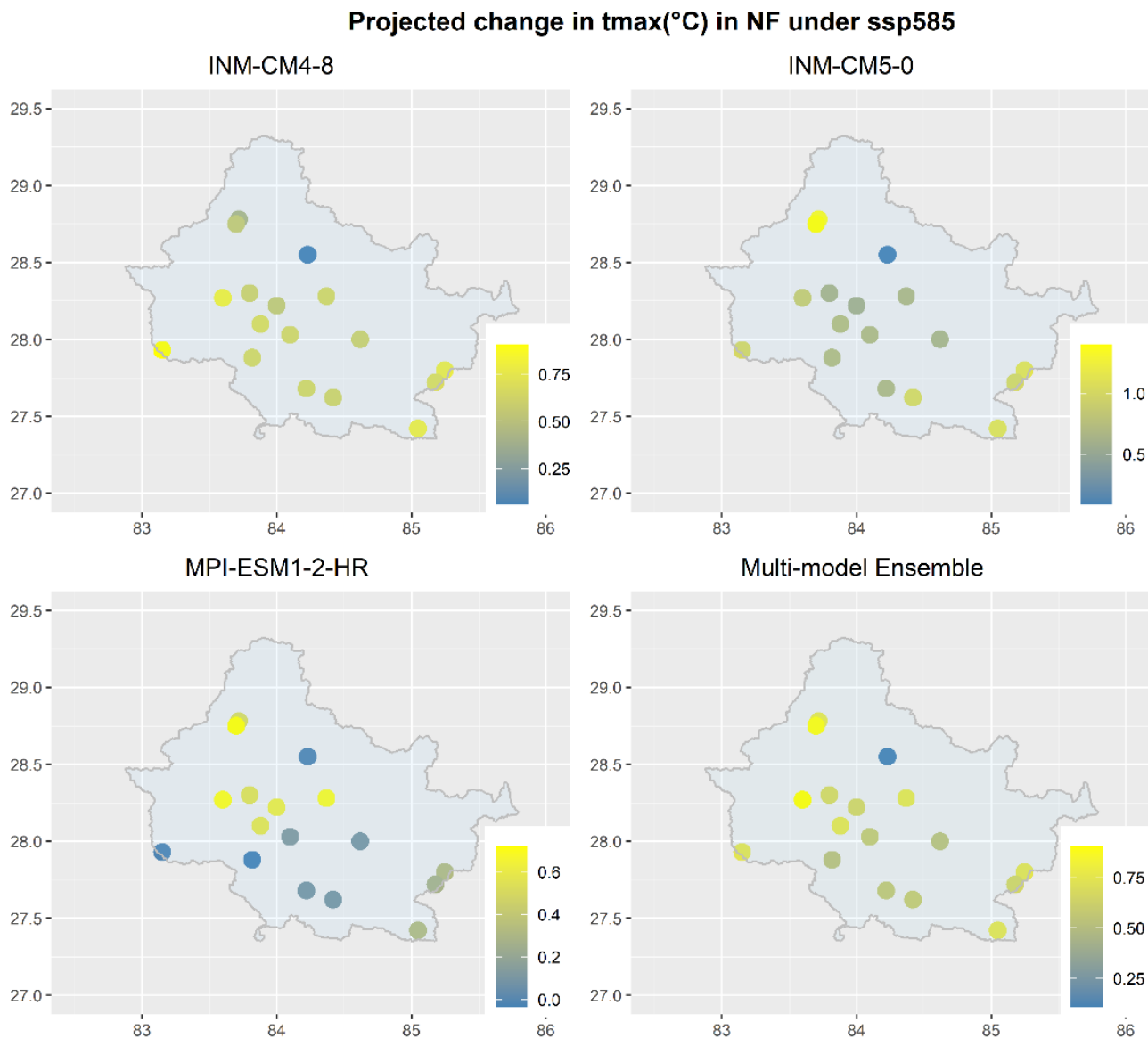


Figure 7: Projected Change in maximum temperature (°C) in Near Future under ssp245

average annual T_{max} across the NRB is projected to increase ranging from 0.08 °C to 1.09 °C for NF, 0.74 °C to 1.58 °C for MF, and 1.45 °C to 2.15 °C for FF under SSP245. Similarly, under SSP585, the T_{max} will increase ranging from 0.6 °C to 1.40 °C for NF, 1.26 °C to 2.31 °C for MF, and 2.90 °C to 4.68 °C for FF. Similarly for average annual T_{min} is projected to increase by ranging from 0.39° C to 1.24 °C for NF, 1.53 °C to 2.74 °C for MF, and 1.85 °C to 3.20 °C for FF under SSP245. Similarly, under SSP585 the T_{min} will increase ranging from 0.42 °C to 1.46 °C for NF, 2.08 °C to 3.82 °C for MF, and 3.30 °C to 5.22 °C for FF. . Furthermore, varying trends are projected across the seasons; higher change in winter temperature (0.9 °C to 5.4 °C) followed by pre-monsoon (-0.1 °C to 2.8 °C) for T_{max} while winter (0.8 °C to 3.7 °C) followed

by post-monsoon (1.1 °C to 4.1 °C) for T_{min} is observed for three future periods.

The trend analysis of projected future temperature, namely, near (2021-2045), mid (2046-2075), and far (2076-2100), was done using the Mann-Kendall trend test, and the slope of the trend was calculated by Sen's slope for both T_{max} and T_{min} . There is a warming trend in the majority of the stations for T_{max} and T_{min} . The result obtained from trend analysis of mean annual temperature data indicated a significant warming trend in T_{max} and T_{min} . The magnitude of mean annual trend is 0.06°C yr⁻¹ in NF, 0.04°C yr⁻¹ in MF, and 0.02°C yr⁻¹ in FF for T_{max} under SSP245. Similarly, 0.05°C yr⁻¹ in NF, 0.07°C yr⁻¹ in MF, and 0.1°C yr⁻¹ in FF are obtained under SSP585 for T_{max} . Also, the magnitude

of mean annual trend is $0.07^{\circ}\text{C yr}^{-1}$ in NF, $0.04^{\circ}\text{C yr}^{-1}$ in MF, and $0.02^{\circ}\text{C yr}^{-1}$ in FF for T_{\min} under SSP245. Similarly, $0.06^{\circ}\text{C yr}^{-1}$ in NF, $0.07^{\circ}\text{C yr}^{-1}$ in MF, and $0.09^{\circ}\text{C yr}^{-1}$ in FF are obtained under SSP585 for T_{\min} . The result shows that the increasing trend will be more significant for T_{\min} than T_{\max} .

This study suggests that the temperature in the NRB will increase significantly in future. Warming trend is more for the mountainous region, which can considerably affect the snow and glacier cover area. So there will be high influence in runoff and water availability which can cause various hydrological disasters in the basin. Also the winter season will have higher impacts of rising temperature. The proper mitigation and adaptation strategies should be formulated to reduce impacts of warming temperature. The result obtained from this study may be useful for further investigations in future climate and hydrology of the basin.

References

- [1] J. Hansen, R. Ruedy, M. Sato, and K. Lo. Global surface temperature change. *Reviews of Geophysics*, 48(4):1–29, 2010.
- [2] IPCC. Climate Change 2014. *Climate Change 2014: Synthesis Report*, 1(October):1–169, 2014.
- [3] Vishnu Prasad Pandey, Mukand S. Babel, Sangam Shrestha, and Futaba Kazama. A framework to assess adaptive capacity of the water resources system in Nepalese river basins. *Ecological Indicators*, 11(2):480–488, 2011.
- [4] Lin Wang and Wen Chen. A CMIP5 multimodel projection of future temperature, precipitation, and climatological drought in China. *International Journal of Climatology*, 34(6):2059–2078, 2014.
- [5] Mansour Almazroui, Sajjad Saeed, Fahad Saeed, M. Nazrul Islam, and Muhammad Ismail. Projections of Precipitation and Temperature over the South Asian Countries in CMIP6. *Earth Systems and Environment*, 4(2):297–320, 2020.
- [6] Anshul Agarwal, Mukand S. Babel, Shreedhar Maskey, Sangam Shrestha, Akiyuki Kawasaki, and Nitin K. Tripathi. Analysis of temperature projections in the Koshi River Basin, Nepal. *International Journal of Climatology*, 36(1):266–279, 2016.
- [7] Laxmi Prasad Devkota and Dhiraj Raj Gyawali. Impacts of climate change on hydrological regime and water resources management of the Koshi River Basin, Nepal. *Journal of Hydrology: Regional Studies*, 4:502–515, 2015.
- [8] S. Nepal, P. Krause, W. A. Flügel, M. Fink, and C. Fischer. Understanding the hydrological system dynamics of a glaciated alpine catchment in the Himalayan region using the J2000 hydrological model. *Hydrological Processes*, 28(3):1329–1344, 2014.
- [9] Piyush Dahal, Madan Lall Shrestha, Jeeban Panthi, and Dhiraj Pradhananga. Modeling the future impacts of climate change on water availability in the Karnali River Basin of Nepal Himalaya. *Environmental Research*, 185(February):109430, 2020.
- [10] V. Dahal, N. M. Shakya, and R. Bhattarai. Estimating the Impact of Climate Change on Water Availability in Bagmati Basin, Nepal. *Environmental Processes*, 3(1):1–17, 2016.
- [11] Santosh Kaini, Santosh Nepal, Saurav Pradhananga, Ted Gardner, and Ashok K. Sharma. Representative general circulation models selection and downscaling of climate data for the transboundary Koshi river basin in China and Nepal. *International Journal of Climatology*, 40(9):4131–4149, 2020.
- [12] Rupak Rajbhandari, Arun Bhakta Shrestha, Santosh Nepal, and Shahriar Wahid. Projection of Future Climate over the Koshi River Basin Based on CMIP5 GCMs. *Atmospheric and Climate Sciences*, 06(02):190–204, 2016.
- [13] Sanita Dhaubanjari, Vishnu Prasad Pandey, and Luna Bharati. Climate futures for Western Nepal based on regional climate models in the CORDEX-SA. *International Journal of Climatology*, 40(4):2201–2225, 2020.
- [14] Mohan Chand, Bikas Bhattarai, Prashant Baral, and Niraj Pradhananga. Trend Analysis of Temperature Data for Narayani River Basin, Nepal. *Sci*, 1(1):21, 2019.
- [15] Prashant Baral, Rijan B. Kayastha, Walter W. Immerzeel, Niraj S. Pradhananga, Bikas C. Bhattarai, Sonika Shahi, Stephan Galos, Claudia Springer, Sharad P. Joshi, and Pradeep K. Mool. Preliminary results of mass-balance observations of Yala Glacier and analysis of temperature and precipitation gradients in Langtang Valley, Nepal. *Annals of Glaciology*, 55(66):9–14, 2014.
- [16] Marielle Saunio, Ann Stavert, Ben Poulter, Philippe Bousquet, Robert Jackson, Peter Raymond, Edward Dlugokencky, Prabir Patra, Marielle Saunio, Ann Stavert, Ben Poulter, Philippe Bousquet, Josep Canadell, The Global, Marielle Saunio, Ann R Stavert, Ben Poulter, Philippe Bousquet, and Josep G Canadell. The Global Methane Budget 2000 – 2017 To cite this version : HAL Id : hal-02969930 The Global Methane Budget 2000 – 2017. 2020.
- [17] Arthur F. Lutz, Herbert W. ter Maat, Hester Biemans, Arun B. Shrestha, Philippus Wester, and Walter W. Immerzeel. Selecting representative climate models for climate change impact studies: an advanced envelope-based selection approach. *International Journal of Climatology*, 36(12):3988–4005, 2016.
- [18] Najeebullah Khan, Shamsuddin Shahid, Kamal Ahmed, Tarmizi Ismail, Nadeem Nawaz, and Minwoo Son. Performance assessment of general circulation model in simulating daily precipitation and temperature using multiple gridded datasets. *Water (Switzerland)*, 10(12), 2018.
- [19] Claudia Teutschbein and Jan Seibert. University of Zurich Zurich Open Repository and Archive Regional climate models for hydrological impact studies at the catchment scale : a review of recent modeling

- strategies Regional Climate Models for Hydrological Impact Studies at the Catchment-Scale. *Geography Compass*, 4(7):834–860, 2010.
- [20] Enrique Soriano, Luis Mediero, and Carlos Garijo. Selection of bias correction methods to assess the impact of climate change on flood frequency curves. *Water (Switzerland)*, 11(11), 2019.
- [21] Deo Raj Gurung, Sudan Bikash Maharjan, Anu Bhalu Shrestha, Mandira Singh Shrestha, Sagar Ratna Bajracharya, and M. S.R. Murthy. Climate and topographic controls on snow cover dynamics in the Hindu Kush Himalaya. *International Journal of Climatology*, 37(10):3873–3882, 2017.
- [22] Piyush Dahal, Nicky Shree Shrestha, Madan Lall Shrestha, Nir Y. Krakauer, Jeeban Panthi, Soni M. Pradhanang, Ajay Jha, and Tarendra Lakhankar. Drought risk assessment in central Nepal: temporal and spatial analysis. *Natural Hazards*, 80(3):1913–1932, 2016.
- [23] Matthew J. Gidden, Keywan Riahi, Steven J. Smith, Shinichiro Fujimori, Gunnar Luderer, Elmar Kriegler, Detlef P. Van Vuuren, Maarten Van Den Berg, Leyang Feng, David Klein, Katherine Calvin, Jonathan C. Doelman, Stefan Frank, Oliver Fricko, Mathijs Harmsen, Tomoko Hasegawa, Petr Havlik, Jérôme Hilaire, Rachel Hoesly, Jill Horing, Alexander Popp, Elke Stehfest, and Kiyoshi Takahashi. Global emissions pathways under different socioeconomic scenarios for use in CMIP6: A dataset of harmonized emissions trajectories through the end of the century. *Geoscientific Model Development*, 12(4):1443–1475, 2019.
- [24] Akiyo Yatagai, Kenji Kamiguchi, Osamu Arakawa, Atsushi Hamada, Natsuko Yasutomi, and Akio Kitoh. Aphrodite constructing a long-term daily gridded precipitation dataset for Asia based on a dense network of rain gauges. *Bulletin of the American Meteorological Society*, 93(9):1401–1415, 2012.
- [25] Vimal Mishra, Udit Bhatia, and Amar Deep Tiwari. Bias-corrected climate projections from Coupled Model Intercomparison Project-6 (CMIP6) for South Asia. 6(June), 2020.
- [26] D N Moriassi, J G Arnold, M W Van Liew, R L Bingner, R D Harmel, and T L Veith. Model Evaluation Guidelines for Systematic Quantification Of Accuracy in Watershed Simulations. 50(3):885–900, 2007.
- [27] Min Luo, Tie Liu, Fanhao Meng, Yongchao Duan, Amaury Frankl, Anming Bao, and Philippe De Maeyer. Comparing bias correction methods used in downscaling precipitation and temperature from regional climate models: A case study from the Kaidu River Basin in Western China. *Water (Switzerland)*, 10(8), 2018.
- [28] Hayley J. Fowler, S. Blenkinsop, and C. Tebaldi. Linking climate change modelling to impacts studies: Recent advances in downscaling techniques for hydrological modelling. *International Journal of Climatology*, 27(12):1547–1578, 2007.
- [29] D Maraun, S Brienens, H W Rust, T Sauter, M Themeßl, V K C Venema, and K P Chun. Precipitation Downscaling under Climate Change. *October*, (2009):1–34, 2010.
- [30] Lukas Gudmundsson. Technical Note: Downscaling RCM precipitation to the station scale using quantile mapping – a comparison of methods. *Hydrology and Earth System Sciences Discussions*, 9(5):6185–6201, 2012.
- [31] Yuanyuan Zhai, Gordon Huang, Xiuquan Wang, Xiong Zhou, Chen Lu, and Zoe Li. Future projections of temperature changes in Ottawa, Canada through stepwise clustered downscaling of multiple GCMs under RCPs. *Climate Dynamics*, 52(5-6):3455–3470, 2019.
- [32] C. Piani, G. P. Weedon, M. Best, S. M. Gomes, P. Viterbo, S. Hagemann, and J. O. Haerter. Statistical bias correction of global simulated daily precipitation and temperature for the application of hydrological models. *Journal of Hydrology*, 395(3-4):199–215, 2010.
- [33] Vishnu Prasad Pandey, Sanita Dhaubanjari, Luna Bharati, and Bhesh Raj Thapa. Hydrological response of Chamelia watershed in Mahakali Basin to climate change. *Science of the Total Environment*, 650:365–383, 2019.
- [34] Ramchandra Karki, Shabeh ul Hasson, Lars Gerlitz, Rocky Talchabhadel, Udo Schickhoff, Thomas Scholten, and Jürgen Böhner. Rising mean and extreme near-surface air temperature across Nepal. *International Journal of Climatology*, 40(4):2445–2463, 2020.
- [35] Pranab Kumar Sen. Journal of the American Statistical Estimates of the Regression Coefficient Based on Kendall’s Tau. *Journal of the American Statistical Association*, 63(324):1379–1389, 1968.
- [36] Asad Amin, Wajid Nasim, Shah Fahad, Shaukat Ali, Shakeel Ahmad, Atta Rasool, Nadia Saleem, Hafiz Mohkum Hammad, Syeda Refat Sultana, Muhammad Mubeen, Hafiz Faiq Bakhat, Naveed Ahmad, Ghulam Mustafa Shah, Muhammad Adnan, Muhammad Noor, Abdul Basir, Shah Saud, Muhammad Habib ur Rahman, and Joel O. Paz. Evaluation and analysis of temperature for historical (1996–2015) and projected (2030–2060) climates in Pakistan using SimCLIM climate model: Ensemble application. *Atmospheric Research*, 213:422–436, 2018.
- [37] Milan Gocic and Slavisa Trajkovic. Analysis of changes in meteorological variables using Mann-Kendall and Sen’s slope estimator statistical tests in Serbia. *Global and Planetary Change*, 100:172–182, 2013.